Threshold for Primordial Black Hole Formation

Adam Mendoza

Gravity Group
GANAP Research Laboratory
National Institute of Physics

The paper

PHYSICAL REVIEW D **100,** 123524 (2019)

Editors' Suggestion

Threshold for primordial black holes: Dependence on the shape of the cosmological perturbations

Ilia Musco*

Institut de Ciències del Cosmos, Universitat de Barcelona, Martí i Franquès 1, 08028 Barcelona, Spain; Laboratoire Univers et Théories, UMR 8102 CNRS, Observatoire de Paris, Université Paris Diderot, 5 Place Jules Janssen, F-92190 Meudon, France, and Département de Physique Théorique, Université de Genève, 24 quai E. Ansermet, CH-1211 Geneva, Switzerland

(Received 29 October 2019; published 16 December 2019)

Primordial black holes may have formed in the radiative era of the early Universe from the collapse of large enough amplitude perturbations of the metric. These correspond to non linear energy density perturbations characterized by an amplitude larger than a certain threshold, measured when the perturbations reenter the cosmological horizon. The process of primordial black hole formation is studied here within spherical symmetry, using the gradient expansion approximation in the long wavelength limit, where the pressure gradients are small, and the initial perturbations are functions only of a time-independent curvature profile. In this regime it is possible to understand how the threshold for primordial black hole formation depends on the shape of the initial energy density profile, clarifying the relation between local and averaged measures of the perturbation amplitude. Although there is no universal

Outline

- Primordial black holes as a consequence of inflationary perturbations
- Mechanism for primordial black hole formation
- Constructing a consistent set of initial conditions for numerical implementation
- Dependence of formation threshold on the shape of curvature perturbation

Primordial black holes

- Primordial black holes are formed in the early universe (during the radiation and matter-dominated eras) due to the gravitational collapse of cosmological perturbations generated before inflation, provided that they exceed a mass/density threshold.
- Due to the nature of its formation, it can assume a wide range of masses.

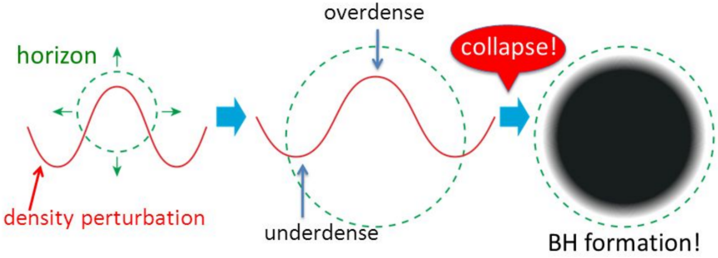

Primordial black holes

- The existence of primordial black holes may, according to Escriva (2024) [1], explain the following:
  1. Microlensing events in the Galactic bulge from planetary-mass objects exceeding free-floating planet expectations.
  2. Quasar microlensing in misaligned systems with low stellar lensing probability.
  3. Excess microlensing events from dark objects in the 2–5 $M_{\odot}$ mass gap, where stellar evolution models don't predict black holes.
  4. Absence of ultrafaint dwarf galaxies below a critical radius.
  5. Discovery of high-redshift galaxies ($z > 10$, possibly $z \approx 18$), challenging standard dark matter models.

Primordial black holes

- Constraints on $f(M) \equiv \Omega_{\rm PBH}/\Omega_{\rm CDM}$ from evaporation (red), lensing (magenta), dynamical effects (green), gravitational waves (black), accretion (light blue), CMB distortions (orange), large-scale structure (dark blue) and background effects (grey).
- PBHs can constitute all of the dark matter in the following mass windows:
  - $M \sim 10^{-16} M_\odot - 10^{-11} M_\odot$
  - $M \sim 10^{14} M_\odot - 10^{17} M_\odot$

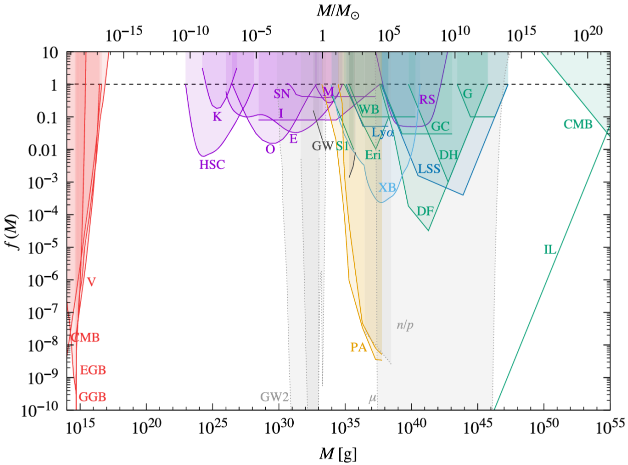

Figure: Constraints on fractions of PBHs as dark matter. Taken from Carr (2021) [2].

Primordial inhomogeneities

- **Before inflation**: perturbations are generated in the inflaton field.
- **During inflation**: the Hubble radius remains nearly constant while comoving scales grow, leading to horizon exit. Curvature perturbations are "frozen" outside the horizon.
- **After inflation**: R_H grows, allowing fluctuation modes to re-enter the horizon during the radiation-dominated (RD) and matter-dominated (MD) eras.

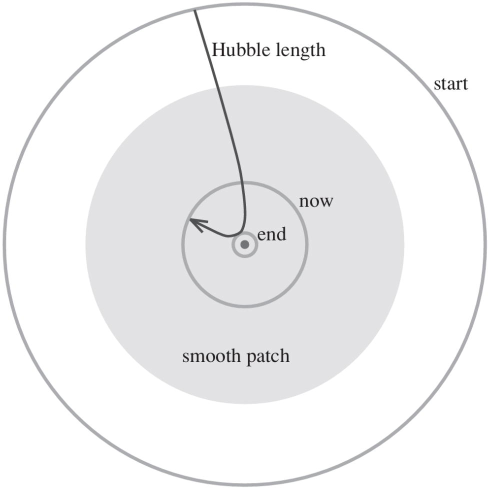

Primordial inhomogeneities

- **Before inflation**: perturbations are generated in the inflaton field.
- **During inflation**: the Hubble radius remains nearly constant while comoving scales grow, leading to horizon exit. Curvature perturbations are "frozen" outside the horizon.
- **After inflation**: R_H grows, allowing fluctuation modes to re-enter the horizon during the radiation-dominated (RD) and matter-dominated (MD) eras.

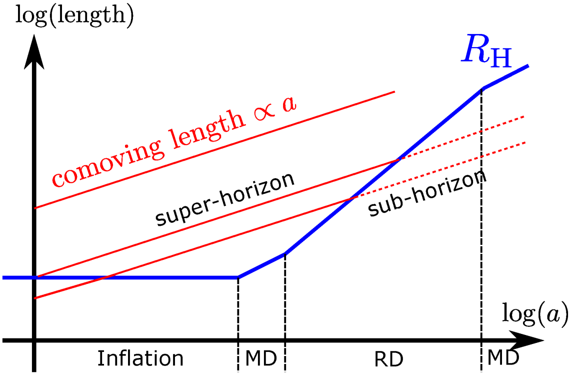

Primordial inhomogeneities

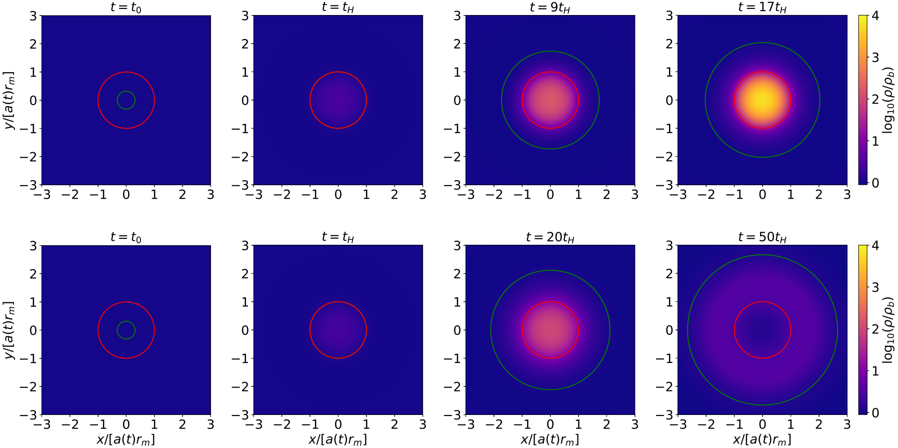

Time evolution of supercritical and subcritical Gaussian density fluctuation [1].

Harada-Yoo-Kohri threshold

- Overdense region initially expands and may eventually reach a maximum expansion.
- If pressure waves reach the edge of the overdensity before maximum expansion, collapse will be significantly delayed.
- Threshold, $\delta \equiv (\rho - \rho_b)/\rho_b$:

$$\delta_c = \frac{3(1+w)}{5+3w} \sin^2\left(\frac{\pi\sqrt{w}}{1+3w}\right) \qquad (1)$$

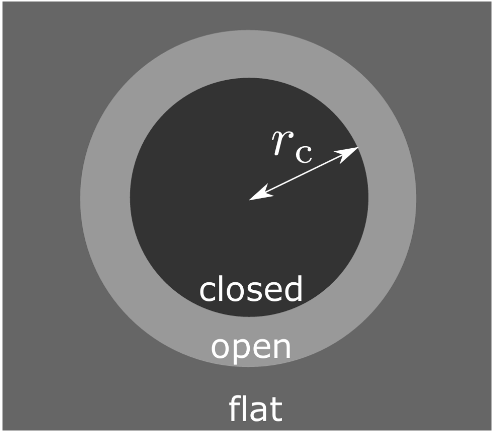

Figure: Harada's three-zone model

Harada-Yoo-Kohri threshold

- Overdense region initially expands and may eventually reach a maximum expansion.
- If pressure waves reach the edge of the overdensity before maximum expansion, collapse will be significantly delayed.
- Threshold, $\delta \equiv (\rho - \rho_b)/\rho_b$:

$$\delta_c = \frac{3(1+w)}{5+3w} \sin^2\left(\frac{\pi\sqrt{w}}{1+3w}\right) \qquad (1)$$

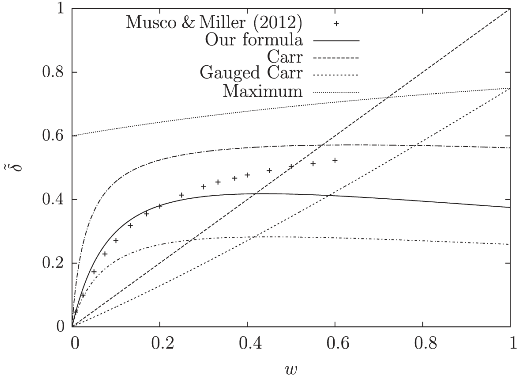

Figure: Comparison with numerical results

Misner-Sharp-Hernandez equations

- In the comoving gauge, we are given a general, spherically symmetric metric of the form

$$\mathrm{d}s^2 = -A^2(r,t)\,\mathrm{d}t^2 + B^2(r,t)\,\mathrm{d}r^2 + R^2(r,t)\,\mathrm{d}\Omega^2. \tag{2}$$

  and the stress-energy tensor

$$T^{\mu\nu} = (\rho + P)\,u^\mu u^\nu + P g^{\mu\nu} \tag{3}$$

  where $u^\mu = n^\mu = (1/A, 0, 0, 0)$.

- Define

$$\mathrm{D}_t \equiv \frac{1}{A}\frac{\partial}{\partial t} \tag{4}$$

$$\mathrm{D}_r \equiv \frac{1}{B}\frac{\partial}{\partial r} \tag{5}$$

$$U \equiv D_t R = \frac{1}{A}\frac{\partial R}{\partial t} \tag{6}$$

$$\Gamma \equiv D_r R = \frac{1}{B}\frac{\partial R}{\partial r} \tag{7}$$

Misner-Sharp-Hernandez equations

- Given the spherically symmetric metric ansatz and the stress-energy tensor in the comoving gauge, the Misner-Sharp-Hernandez (MSH) equations read as

$$\Gamma^2 = 1 + U^2 - \frac{2M}{R} \tag{8}$$

$$M = \int_0^R 4\pi R^2 \rho \, \mathrm{d}R \tag{9}$$

$$\mathrm{D}_t \Gamma = -\frac{U}{e + P} \mathrm{D}_r P \tag{10}$$

$$\mathrm{D}_r M = 4\pi R^2 \Gamma \rho \tag{11}$$

$$\mathrm{D}_t M = -4\pi R^2 U P \tag{12}$$

$$\mathrm{D}_t U = -\frac{\Gamma}{\rho + P} D_r P - \frac{M}{R^2} - 4\pi R P \tag{13}$$

$$\mathrm{D}_t \rho_0 = -\frac{\rho_0}{\Gamma R^2} D_r(R^2 U) \tag{14}$$

$$\mathrm{D}_t \rho = \frac{\rho + P}{\rho_0} D_t \rho_0 \tag{15}$$

$$\mathrm{D}_r A = -\frac{A}{\rho + P} D_r P \tag{16}$$

where $\rho = \rho_0(1 + e)$ where ρ_0 is the rest mass density and e is the internal energy density.

Black hole formation

- For the Misner-Sharp mass, M, and the areal radius R, the following relation holds:

$$\frac{2M}{R} = 1 - g^{ab}\nabla_a R \nabla_b R. \tag{17}$$

- If the peak of $2M/R$ reaches 1, then a black hole forms.

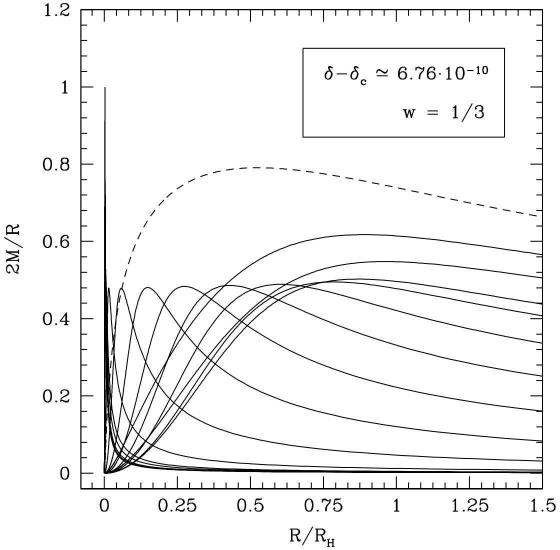

Threshold determination scheme

- Set initial conditions and the initial density contrast/mass excess, δ.
- Evolve using the Misner-Sharp-Hernandez equations.
- Repeat for a different δ.
- Find the perturbation threshold δ_c which marks the boundary between δ that leads to the formation of black holes and δ that does not.

ADM Formalism

- We take the $(3+1)$ decomposition of the metric as a starting point:

$$\mathrm{d}s^2 = -\alpha^2\,\mathrm{d}t^2 + \gamma_{ij}\left(\mathrm{d}x^i + \beta^i\,\mathrm{d}t\right)\left(\mathrm{d}x^j + \beta^j\,\mathrm{d}t\right). \tag{18}$$

  The functions α, β^i, and γ_{ij} are the lapse function, shift vector, and the spatial metric, respectively.

- In general, the 3-metric can be decomposed in the following manner:

$$\gamma_{ij} \equiv a^2(t)e^{2\zeta(t,x^i)}\bar{\gamma}_{ij}. \tag{19}$$

  Here, $a(t)$ is the global scale factor, $\zeta(t,x^i)$ is a "curvature perturbation", $\bar{\gamma}_{ij}$ is time-independent, and $\det[\bar{\gamma}_{ij}] = 1$.

Long wavelength approximation

- Define a small parameter $\epsilon \equiv R_H/L$ where R_H is the Hubble radius, $R_H = 1/H$, and L is the lengthscale of the perturbation.
- Multiply each spatial gradient by ϵ, $\partial_i \to \epsilon\partial_i$, and expand the equations in ϵ up to the first non-zero order.
- In this formalism, it is always possible to find a coordinate system where the metric of any local region can be written as

$$\mathrm{d}s^2 = -\mathrm{d}t^2 + a^2(t)\,\delta_{ij}\,\mathrm{d}x^i\mathrm{d}x^j. \tag{20}$$

- If we want to recover the local metric in the limit where $\epsilon \to 0$ and if we neglect decaying terms, Lyth et al. [3] showed that $\beta_i = \mathcal{O}(\epsilon)$, $\alpha = 1 + \mathcal{O}(\epsilon^2)$, $\bar{\gamma}_{ij} = \delta_{ij} + \mathcal{O}(\epsilon^2)$, and $\partial_t\zeta = \mathcal{O}(\epsilon^2)$.

Curvature perturbation

- Consider the general scalar perturbation of the metric components (in first order) is given by:

$$\mathrm{d}s^2 = a^2 \left[-\left(1+2A\right)\, \mathrm{d}\eta^2 + 2\partial_i B \, \mathrm{d}\eta \, \mathrm{d}x^i + \left[(1+2C)\delta_{ij} + 2\partial_{\langle i}\partial_{j\rangle} E \right] \mathrm{d}x^i \mathrm{d}x^j \right] \tag{21}$$

where $\mathrm{d}\eta \equiv \mathrm{d}t/a(t)$ and $\partial_{\langle i}\partial_{j\rangle} = \left(\partial_i\partial_j - \frac{1}{3}\boldsymbol{\nabla}^2\right) E$.

- One gauge invariant quantity

$$\zeta_L \equiv C - \frac{1}{3}\boldsymbol{\nabla}^2 E + \mathcal{H}(v+B) \tag{22}$$

is called a *curvature perturbation* due to its relation with the curvature of the constant-time slices:

$$a^2 R_{(3)} = -4\boldsymbol{\nabla}^2 \left(C - \frac{1}{3}\boldsymbol{\nabla}^2 E \right). \tag{23}$$

Curvature perturbation

- In the comoving gauge where $v = B = E = 0$, the metric assumes the form

$$\mathrm{d}s^2 = -(1+2A)\,\mathrm{d}t^2 + a^2(t)(1+2\zeta_L)\delta_{ij}\,\mathrm{d}x^i\mathrm{d}x^j. \tag{24}$$

- We can see that our ζ coincides with ζ_L at linear order, and we allow our ζ to be designated as **curvature perturbation**.
- In the long wavelength approach, we write the metric as

$$\mathrm{d}s^2 = -\mathrm{d}t^2 + a^2(t)e^{2\zeta(\hat{r})}\left[\mathrm{d}\hat{r}^2 + \hat{r}^2\,\mathrm{d}\Omega^2\right] \tag{25}$$

which is equivalent to

$$\mathrm{d}s^2 = -\mathrm{d}t^2 + a^2(t)\left[\frac{\mathrm{d}r^2}{1-K(r)\,r^2} + r^2\,\mathrm{d}\Omega^2\right]. \tag{26}$$

Quasi-homogeneous solution

- Solve the MSH equations in the long-wavelength approximation, given the equation of state $P = w\rho$.
- We expand the metric components up to the first non-zero order:

$$A = 1 + \epsilon^2 \tilde{A} \tag{27}$$

$$B = \frac{R'}{\sqrt{1 - K(r)r^2}} \left(1 + \epsilon^2 \tilde{B}\right) \tag{28}$$

$$R = a(t)r \left(1 + \epsilon^2 \tilde{R}\right) \tag{29}$$

- MSH allows us to expand the hydrodynamical variables as

$$\rho = \rho_b(t) \left(1 + \epsilon^2 \tilde{\rho}\right) \tag{30}$$

$$U = H(t)R \left(1 + \epsilon^2 \tilde{U}\right) \tag{31}$$

$$M = \frac{4\pi}{3} \rho_b(t) R^3 \left(1 + \epsilon^2 \tilde{M}\right). \tag{32}$$

Quasi-homogeneous solution

- The tilde variables were shown to have the form [4]:

$$\tilde{\rho} = \frac{3(1+w)}{5+3w}\left[K(r) + \frac{1}{3}rK'(r)\right] r_k^2 \tag{33}$$

$$\tilde{U} = -\frac{1}{5+3w}K(r)r_k^2 \tag{34}$$

$$\tilde{A} = -\frac{w}{1+w}\tilde{\rho} \tag{35}$$

$$\tilde{M} = -3(1+w)\tilde{U} \tag{36}$$

$$\tilde{R} = -\frac{w}{(1+3w)(1+w)}\tilde{\rho} + \frac{1}{1+3w}\tilde{U} \tag{37}$$

$$\tilde{B} = \frac{w}{(1+3w)(1+w)} r\frac{d\tilde{\rho}}{dr} \tag{38}$$

The perturbation amplitude

- Define the averaged mass excess

$$\delta(r, t) \equiv \frac{1}{V} \int_0^R 4\pi R^2 \frac{\rho - \rho_b}{\rho_b} \, \mathrm{d}R \tag{39}$$

where $V = 4\pi R^3/3$. At the long-wavelength approximation,

$$\delta(r, t) = \frac{3}{r^3} \int_0^r \frac{\delta\rho}{\rho_b} r^2 \, \mathrm{d}r = \epsilon^2(t) f(w) K(r) r_k^2 = \epsilon^2 \tilde{M}. \tag{40}$$

where $f(w) = 3(1+w)/(5+3w)$.

- We can give $K(r)$ the physical interpretation that it is proportional to the averaged mass excess within a sphere of comoving radius r.

Compaction function

- We define the compaction function as

$$\mathcal{C} \equiv \frac{2\left[M(r,t) - M_b(r,t)\right]}{R(r,t)} \approx \frac{r^2}{r_k^2}\tilde{M} + \mathcal{O}(\epsilon^2) \tag{41}$$

where the weak equality is the long-wavelength approximation. Using the equation for $\tilde{M}$, we can express the approximation for the compaction function as

$$\mathcal{C}(r) = \frac{r^2}{r_k^2}\tilde{M} = f(w)K(r)r^2 = \frac{r^2}{r_k^2}\delta(r) \tag{42}$$

Identifying the lengthscale of the perturbation with the location of the maximum of the compaction function, r_m, gives us the relation

$$\delta(r_m, t) = 3\frac{\delta\rho(r_m, t)}{\rho_b(t)}. \tag{43}$$

Compensated perturbation profiles

- Consider a Gaussian curvature profile

$$K(r) = \left(\frac{r}{\Delta}\right)^{2\lambda} \mathcal{A} \exp\left[-\frac{1}{2}\left(\frac{r}{\Delta}\right)^{2\alpha}\right] \tag{44}$$

- The following quantities can be derived:

$$\frac{\delta\rho}{\rho_b} = \left(\frac{1}{aH}\right)^2 f(w)\left[1 + \frac{2\lambda}{3} - \frac{\alpha}{2}\left(\frac{r}{\Delta}\right)^{2\alpha}\right] K(r) \tag{45}$$

$$\frac{r_0}{r_m} = \left[\frac{2\lambda + 3}{2(\lambda + 1)}\right]^{1/2\alpha} \tag{46}$$

where r_0 is located at $\delta\rho/\rho_b = 0$ and r_m is the location of the maximum of the compaction function.

Compensated perturbation profiles

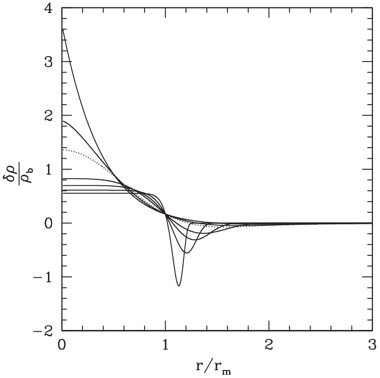

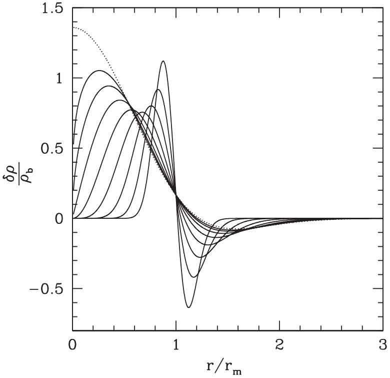

Increasing α creates flatter density contrast. Increasing λ shifts the density contrast to the right.

Threshold determination scheme

- Specify initial data at $ar \gg R_H$ through the curvature profile, and specify δ_m at horizon crossing, $\epsilon = 1$.
- Evolve using the Misner-Sharp-Hernandez equations.
- Check if PBH forms or not.
- Repeat for different δ_m, α and λ.
- Determine $\delta_{m,c}$.

Results

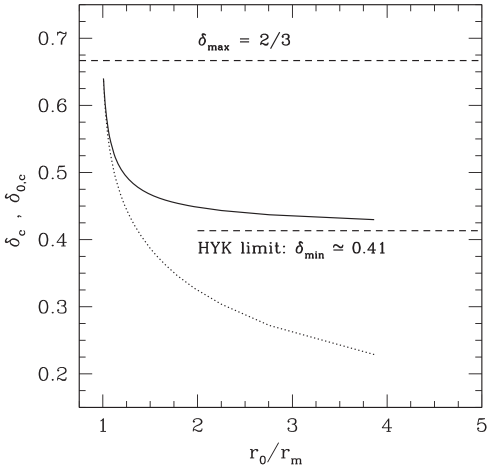

- Behavior of δ_c (solid), evaluated at r_m, and $\delta_{0,c}$ (dashed), evaluated at r_0, with respect to r_0/r_m.
- Sharper profiles form PBHs easily compared to flatter profiles.
- Musco argued that r_m is the preferable evaluation point due to the density contrast-mass excess relation derived earlier.
- Recall:

$$\frac{r_0}{r_m} = \left[\frac{2\lambda + 3}{2(\lambda + 1)}\right]^{1/2\alpha}$$

Results

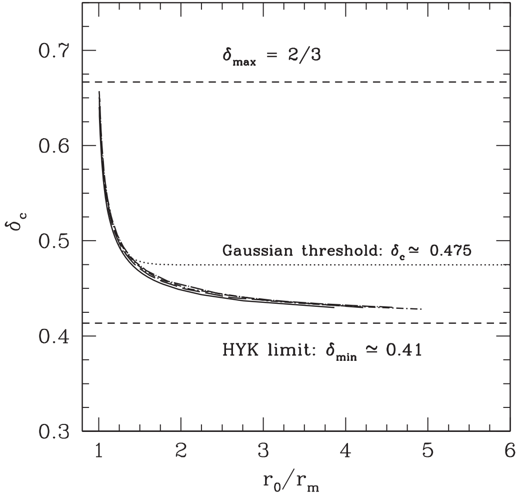

- Different λ values were considered, but they give the same threshold curve.
- Off-centered profiles, $\lambda \neq 0$, were found to redistribute, converging towards a centrally peaked profile with the same amplitude.
- Ultimately, α, and equivalently r_0/r_m matters, more than the location of the peak.
- Recall:

$$\frac{r_0}{r_m} = \left[\frac{2\lambda + 3}{2(\lambda + 1)}\right]^{1/2\alpha}$$

Conclusions

- The maximum of the compaction allows for a simple relation between a "global" value, δ, and a "local" value, $\delta\rho/\rho_b$:

$$\delta(r_m, t) = 3\frac{\delta\rho(r_m, t)}{\rho_b(t)}. \tag{47}$$

- The threshold primarily depends on the sharpness of the profile. Profiles with sharply peaked density contrast form PBHs easily compared to flat profiles.
- Broader shapes of density contrast correspond to small pressure gradients, while sharper density contrasts correspond to large pressure gradients.

References I

[1] Albert Escrivà, Florian Kühnel, and Yuichiro Tada. Chapter 4 - Primordial black holes. In Manuel Arca Sedda, Elisa Bortolas, and Mario Spera, editors, *Black Holes in the Era of Gravitational-Wave Astronomy*, pages 261–377. Elsevier, 2024.

[2] Bernard Carr, Kazunori Kohri, Yuuiti Sendouda, and Jun'ichi Yokoyama. Constraints on primordial black holes. *Reports on Progress in Physics*, 84(11):116902, November 2021.

[3] David H Lyth, Karim A Malik, and Misao Sasaki. A general proof of the conservation of the curvature perturbation. *Journal of Cosmology and Astroparticle Physics*, 2005(05):004, May 2005.

[4] Alexander G Polnarev and Ilia Musco. Curvature profiles as initial conditions for primordial black hole formation. *Classical and Quantum Gravity*, 24(6):1405, Mar 2007.